Vertical Accuracy Evaluation of Digital Terrain Model (DTM) ALOS PALSAR-2 in Rote Dead Sea Area – Indonesia

Atriyon JULZARIKA, Trias ADITYA, Subaryono SUBARYONO, Harintaka HARINTAKA – Yogyakarta[1]

ABSTRACT. Vertical accuracy evaluation is essential to determine in order to know the quality of a DTM. This quality will affect the scale type and utilization of the DTM. The study data use DTM ALOS PALSAR-2. This study evaluates the vertical accuracy of the DTM ALOS PALSAR-2 with different height reference fields in the Rote Dead Sea Area, Indonesia. Each DTM is made with the EGM 1996, EGM 2008, and WGM 2012. The three DTMs extracted based on the height reference field will have different orthometric heights; therefore, an evaluation of the vertical accuracy is needed to determine the quality of the three DTMs. They compare with field measurements from GNSS-levelling. This test is carried out at lowland and highland, using 10 test points. For the lowland area, the RMSE (z) in height at DTM is 1.363 m for WGM 2012, 2.017 m for EGM 2008, and 1.934 m for EGM 1996. For the highlands area, the RMSE (z) in height at DTM is 1.185 m for WGM 2012, 1.201 m for EGM 2008, and 1.432 m for EGM 1996. The DTM-WGM 2012 and DTM-EGM 1996 are recommended to use in this area because they have higher vertical accuracy. The vertical accuracy test in the Rote lowland corresponds to class 2 and class 3 on a scale of 1:10,000. The vertical accuracy test results in the Rote highland correspond to class 1 and class 2 on a scale of 1:10,000. The ALOS PALSAR-2 DTM vertical accuracy test results can be used for mapping scales of 1:10,000 – 1:25,000 in Rote.

Keywords: vertical accuracy test, EGM 1996, EGM 2008, WGM 2012, DTM ALOS PALSAR-2.

[1] Atriyon Julzarika, Ph.D. candidate, Department of Geodetic Engineering, Gadjah Mada University, Yogyakarta, Indonesia; Senior Researcher, Indonesian National Institute of Aeronautics and Space (LAPAN), Jakarta, Indonesia, e-mail: verbhakov@yahoo.com

Trias Aditya, Ph.D., Department of Geodetic Engineering, Gadjah Mada University, Yogyakarta, Indonesia, e-mail: triasaditya@ugm.ac.id

Subaryono Subaryono, Ph.D., Department of Geodetic Engineering, Gadjah Mada University, Yogyakarta, Indonesia, e-mail: ssubar@ugm.ac.id

Harintaka Harintaka, Ph.D., Department of Geodetic Engineering, Gadjah Mada University, Yogyakarta, Indonesia, e-mail: harintaka@ugm.ac.id

1. Introduction

The Rote Ndao archipelago is part of East Nusa Tenggara's province, Indonesia's southernmost province (Laksono et al. 2019). Baa is the capital city of Rote Ndao. The Rote Ndao Regency has an area of around 1,731 km². It has 96 islands, only six islands are inhabited. They are Rote, Oesu, Nuse, Ndao, Landu, and Do'o Islands. Geographically, the Rote Ndao is located in 10°25' – 11°15' South Latitude and 121°49' – 123°26' East Longitude, see Fig. 1.

The Eurasian and Indo-Australian plates meet in the archipelago's southern part (Julzarika et al. 2018). On Rote Island, several major faults led to oceanic crust uplifting to form the current landmass. The non-uniform uplift resulted in the creation of many saltwater lakes with unique biodiversity. The Rote Dead Sea area is home to more than 20 saltwater lakes, and in all, a total of over 80 natural and artificial lakes (Julzarika et al. 2018).

DTM data are needed in order to study the unique geology of Rote Ndao. The uniqueness consists of transformations that took place along several faults in the archipelago. The accurate measurement of this deformation is determined by the level of accuracy of the DTM data (Li et al. 2004, Maune and Nayegandhi 2018). As the DTM can be extracted from satellite remote sensing data, one factor that affects its accuracy is the geoid model used for geoid undulation (Krauß 2018, Schuman and Bates 2019).

Much research has been done related to DTMs, including studies related to DTM extraction from optical images, SAR, and video and the DEM fusion and integration (Elkhrachy 2016, Julzarika and Djurdjani 2018). Monserrat et al. (2014) also carried out research related to InSAR for surface deformation. This research's novelty is the study of the vertical accuracy of DTM ALOS PALSAR-2 based on the different height reference files of EGM 1996, EGM 2008, and WGM 2012 for the Rote Dead Sea area. Deformation in Rote was in the form of mixed deformation, which took place due to a combination of Indo-Australian and Eurasian plate movements and the Flores Fault and minor faults in Rote Ndao. Research related to geological uniqueness, DTM, and deformation in Rote Ndao has been scarce and seldom published.
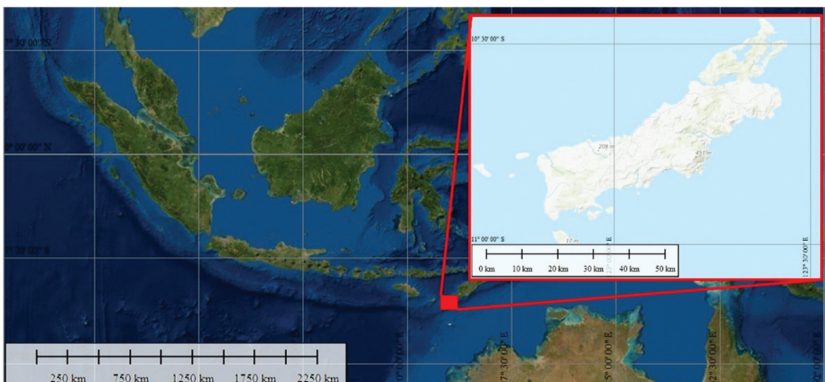

Fig. 1. *Rote dead sea area in Rote islands, Indonesia. The box is the study area.*

This study evaluates the vertical accuracy of DTM ALOS PALSAR-2 with various height reference fields of EGM 1996, EGM 2008, and WGM 2012 for Indonesia's Rote Dead Sea area.

1.1. Geodynamics in Rote island

A fault is a planar fracture or discontinuity in a volume of rock that has significant displacement due to rock-mass movement (Lanari et al. 2004). Faults occur in rocks that experience low pressure and temperature sufficient to make them fragile (Turcotte and Schubert 2014). Significantly large faults result from the action of tectonic plate forces (Venera et al. 2016). This condition will form the boundaries between plates, such as subduction zones (transform faults) (Szostak-Chrzanowski 2006). Earthquakes occur due to the energy released inactive faults' rapid movement (Turcotte and Schubert 2014).

The oldest rock exposed in Rote Ndao is the Aitutu Formation (Julzarika et al. 2018). This formation is a thin interchange of siltstone of various colors (red, brown, grey, greenish) with marl and limestone. The upper part of this formation consists of a layer of white-yellowish calcilutite containing calcite veins with grey flakes. In this formation, a Halobia sp. and Monotis Salinaria fossils have been found in reddish-brown siltstone. The Aitutu Formation is estimated to be of the Late Triassic age (235–208 million years ago). The Aitutu is exposed in the Namodale region, which is part of the Rote Dead Sea area and Timor Leste; its thickness is estimated at 1,000 m (Julzarika et al. 2018).

The Wailuli Formation is located above the Aitutu (Laksono et al. 2019). This formation consists of calcarenite, silt flakes, napal (clay), and greywacke, which are generally grey to greenish. The rock layers have not experienced intense deformation. This formation contains Belemnopsis sp. of the Late Jurassic (157–145 million years ago); it is located in the Oitbolan area, west of Kolbano, West Timor, reaching 450 m in thickness.

The formation above the Wailuli is the Nakfunu formation (Julzarika et al. 2018). This formation consists of siltstone, which contains Radiolaria fossils, flakes with Radiolaria, silt marl, Radiolaria girdle, and calcilutite. This formation's age is thought to be Early Cretaceous (Albian, or 112–97 million years ago), and its thickness reaches 600 m. All these rock formations are covered by younger rocks, consisting of coral reefs (Laksono et al. 2019).

2. Materials and Methods

The data used in this study are ALOS PALSAR-2 imagery for DTM extraction and Global Navigation Satellite System (GNSS)-leveling measurements for DTM vertical accuracy testing. This research using the ALOS PALSAR-2 in January 2018. The field measurement using GNSS-levelling in August 2018. The method used is Interferometry Synthetic Aperture Radar (InSAR) for DTM extraction, while the accuracy-test uses the high-difference test and vertical-accuracy test.

2.1. ALOS PALSAR-2

ALOS PALSAR is a SAR image. ALOS PALSAR satellites were operational in 2006–2011, and ALOS PALSAR-2 has been operational since 2015 (Eorc-JAXA 2018). This SAR satellite emits microwaves and receives reflections from the ground for information (Eorc-JAXA 2018). Fig. 2 is the ALOS PALSAR satellite on imagery tracking.
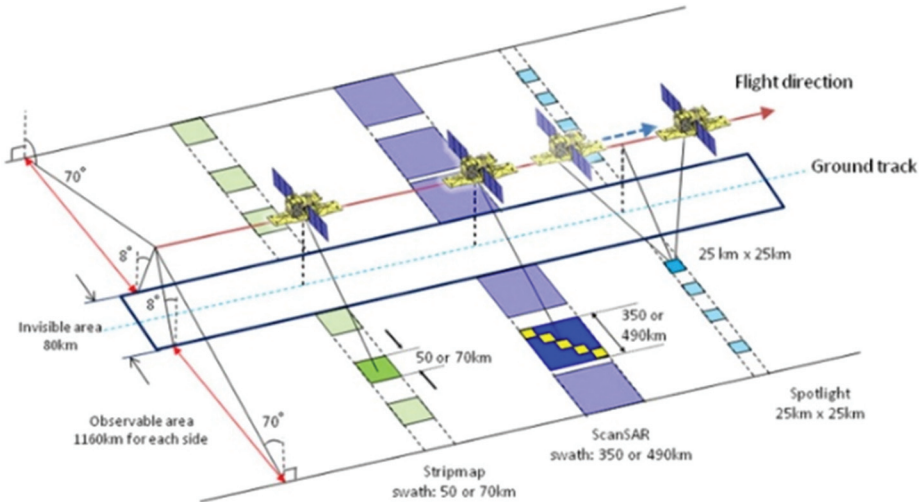

Fig. 2. *ALOS PALSAR satellite on imagery tracking (Eorc-JAXA 2018).*

SAR images have the advantage of providing satellite images regardless of day or night conditions (Lanari et al. 2004). Band L is used as the frequency for sending and receiving microwaves that are not affected by clouds and rain; this capability makes it suitable for rapid disaster monitoring. L-band microwaves can also reach the ground partway through the vegetation cover to get vegetation and soil surface information. The DEM generated from the L-band wave is approaching terrain (Champion and Boldo 2006). A slight correction is needed to convert it to DTM.

2.2. InSAR

A Synthetic Aperture Radar (SAR) system records the amplitude and phase of backscattered radar signals (Arai 2019). The phase of each focused SAR image is the sum of three different contributions: the two-way travel path (sensor-target-sensor), the interaction between the incident, and the phase shift induced by the processing system used to focus the image (Reale et al. 2009, Rucci et al. 2012, Devanthéry et al. 2016).

InSAR is based on the operational principles of SAR obtained from antennas and satellites in Earth orbit (Lazecký et al. 2018). InSAR enables 2D radar

images with high-range resolution along the instrumental line of sight and cross-range resolution along the scan direction (Rucci et al. 2012, Devanthéry et al. 2016). Two antennas each transmit and receive microwave signals and calculate the phase difference between measurements made at two different times (Lanari et al. 2004). InSAR makes it easy to calculate all pixels' displacement from the SAR image (Lazecký et al. 2018).

InSAR is a radar technique used in geodesy and remote sensing (Rucci et al. 2012, Drewes et al. 2016). This geodetic method uses two or more SAR images to produce surface deformation information (Maune and Nayegandhi 2018). It uses wave phase differences that return to satellites or aircraft. This technique has the potential to measure millimeter-scale changes in deformation over a range of days to years (Lanari et al. 2004). This surface deformation can be used for geophysical monitoring of phenomena such as earthquakes, volcanoes, landslides, and structural engineering as a method of monitoring land subsidence and structural stability (Gesch et al. 2014, Drewes et al. 2016).

SAR uses the absolute amplitude and phase of the return signal data (NASA 2018). Interferometry uses a differential phase of radiation reflected from several points along the same path or several center phases moved (antennas) on a single path (Devanthéry et al. 2016). Outgoing waves are generated by satellites; the phases of these waves are known and can be compared with the reverse signal phase (Lanari et al. 2004). The return wave phase depends on the distance to the ground. It is caused by the length of the path to the ground, and the distance to the ground and back will consist of a whole number of wavelengths plus several fractions of the wavelength (Lazecký et al. 2018). This condition can be observed as a phase difference or phase shift in a back wave (Rucci et al. 2012). The total distance to the satellite is the sum of all wavelengths based on the time it takes for energy to travel back and forth to the satellite. This condition is an extra fraction of the wavelength that is especially attractive and is measured with high accuracy (Rucci et al. 2012).

2.3. Height reference field

The geoid is a global average sea level model used to measure the precise surface height (Hofmann-Wellenhof and Moritz 2006). The geoid consists of equipotential fields of the Earth's gravitational field that coincide with the global average sea level (Claessens and Hirt 2013). The geoid is used as a reference field to determine the vertical position, height above sea level, and a point on Earth's surface.

Gravity models include geoid, gravity disturbance, gravity anomaly, free air, Bouguer, and vertical deflection (Balmino and Bonvalot 2016). In this research, the geoid model used in the DTM ALOS PALSAR is discussed. This geoid model will determine the vertical accuracy of DTM in high deformation regions such as Rote. This vertical accuracy is tested by comparing the DTM ALOS PALSAR-2 with the results of GNSS-levelling measurements in the field. The height obtained from this GNSS-levelling measurement is orthometric; this is needed to equalize the reference plane (Drewes et al. 2016, Balmino and Bon-

valot 2016). The height value on the DTM is corrected by the geoid undulation of a particular geoid model. In this study, the DTM study uses the EGM96, EGM 2008, and WGM 2012 geoid models.

The height of a point measured by the GNSS is its height above the ellipsoid surface, the ellipsoid of WGS (World Geodetic System) 1984 (Bayoud and Sideris 2003, Zrinjski et al. 2019). Ellipsoid height (h) is not the same as orthometric height (H); see Fig. 3. The orthometric height used for mapping surveys is measured by leveling (Mukherjee et al. 2012). The orthometric height used for mapping surveys is the measurement by leveling. Orthometric height is the height of the point above the geoid measured along the line of gravity passing through that point (Drewes et al. 2016). The ellipsoid height is the height of the point above the ellipsoid calculated along the ellipsoid's regular line through that point (Serrano-Juan et al. 2020).
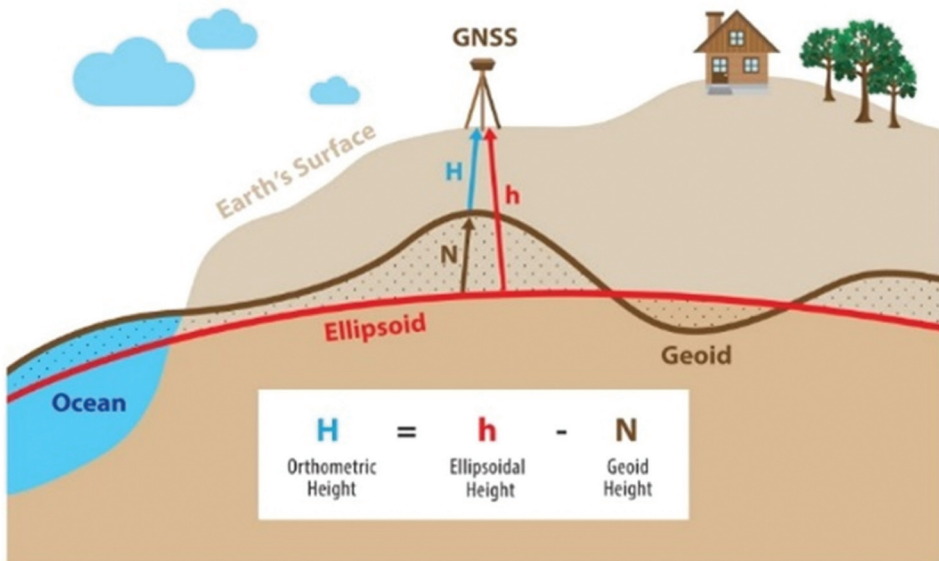

Fig. 3. *Geoid gravity model and its undulation (Albayrak et al. 2020).*

The geoid is one of the equipotential fields of the Earth's gravity field. For practical purposes, geoids are generally considered to coincide with mean sea levels (MSL) (Barthelmes 2013). The geoid is used as a reference field in expressing the orthometric height. Mathematically, a geoid is a highly convoluted surface that requires many parameters to represent its data (Balmino et al. 2012). This mathematical modeling represents the Earth and mathematical calculations (Claessens and Hirt 2013). So far, DSMs and DTMs use reference ellipsoids and not geoids (Satge et al. 2016). Reference ellipsoids and geoids generally do not coincide, and in this case, the geoid height of the ellipsoid is called geoid undulation (N) (Bayoud and Sideris 2003).

GNSS's height is the height of the point above the ellipsoid surface, not the geoid (Albayrak et al. 2020). Geoid undulation is the difference between orthometric height and ellipsoid height. The accuracy of the orthometric height obtained depends on the GNSS's accuracy and the geoid undulation (Balmino and Bonvalot 2016). Precision determination of geoid undulation (to an accuracy on the order of cm) is not an easy job, and detailed gravity data are required, as are high earth topography data and sufficient material density data below the Earth's surface (Bayoud and Sideris 2003, Hirt and Kuhn 2012). The GNSS height transformation to orthometric height is generally carried out with differential data (Balmino et al. 2012). In this research, the geoid models being compared are EGM96, EGM 2008, and WGM 2012.

EGM 1996 is a spherical harmonic model of gravitational potential and was composed of spherical harmonic coefficients complete to degree and order 360 (Barthelmes 2014, Drewes et al. 2016). This model is based on data from around the world in the form of surface gravity data, gravity anomaly data derived from ERS-1 and GEOSAT satellite altimeter data, satellite tracking data (GPS, TDRSS, DORIS, TRANET), and direct altimeter ranges from TOPEX / POSEIDON, ERS-1, and GEOSAT (NASA 2020).

EGM 2008 is a geoid model with free-air gravity anomaly information with a 2.5-minute grid resolution (Barthelmes 2014). The grid is formed from terrestrial data, altimetry derivatives, and gravity data from airborne platforms. EGM2008 was created by the National Geospatial-Intelligence Agency (NGA) and was published in 2008 (Pavlis et al. 2012). This gravity model comprises a complete ball harmonic coefficient with a degree and order value of 2159 and an additional coefficient value of 2190 (Drewes et al. 2016). EGM 2008 illustrates the spherical harmonic model of the Earth's gravitational potential (Barthelmes 2014, ESA 2020). EGM 2008 can be used as the solution for obtaining orthometric height data using the GNSS-levelling measurement method, which is applied primarily at locations far out of reach of the vertical network control distribution (Serrano-Juan et al. 2020).

WGM2012 is the first release of a high-resolution grid and anomaly map of Earth's gravity (Bouguer, isostatic and free-air) calculated globally in spherical geometry (Bonvalot et al. 2012, Barthelmes 2013, Drewes et al. 2016). The gravity anomaly WGM2012 originates from the available global gravity model EGM2008 and DTU10 and includes a 1'x1' resolution field correction derived from the ETOPO1 model (Bonvalot et al. 2012, Barthelmes 2014). WGM2012 considers the contribution of most of the surface mass (oceans, inland seas, lakes, ice caps, land, ice shelves, and atmosphere) (Hirt et al. 2012, Ince et al. 2019). WGM 2012 uses the ball harmonic approach with accurate calculations globally (Bonvalot et al. 2012). For the Indonesian region, gravity values' contribution from local measurements for EGM 1996, EGM 2008, and WGM 2012 is lacking. This condition is caused by the still limited and uneven coverage of geoid measurements for Indonesia. EGM 1996, EGM 2008, and WGM 2012 can be used in determining geoid undulations, and this method can overcome the lack of local geoid measurements in Indonesia.

2.4. DTM extraction

DTM extraction can be done by calculating the tree offset parameter. This parameter is used to convert DSM to DTM with consideration of vegetation height and building height. Tree offset estimation is carried out on the edge of the object with the least-squares approach based on local altitude variation models (Gallant et al. 2012, Maune and Nayegandhi 2018). Correction of height errors is needed to remove altitude errors (Arefi et al. 2009). The artifact is similar to the altitude error in DEM. The correct estimation of tree offset depends on accurately identifying the open field's transition location to the closed field (Gallant et al. 2012). Estimates of tree offsets depend on identifying height objects in topography not covered by the trees (Maune and Nayegandhi 2018).

Offsets that experience altitude errors need to be removed to effectively convert DSM to DTM (Gallant et al. 2012). DSM registration and land cover will result in lower tree offset estimates (Moudrý et al. 2018). DSM SRTM response to tree cover changes is not sharp, but the transition is smooth at a distance of 3-4 cells (about 100 m). This smooth transition must be considered in offset correction to avoid artifacts around the tree cover patch (Mukherjee et al. 2012). DTM is obtained from the reduction of DSM with tree height offsets.

2.5. Vertical accuracy test

This vertical accuracy-test uses the vertical Root Mean Square Error (RMSE (z)) and Accuracy (z) methods (ASPRS 2014, Azeez and Abdulkareem 2019). Height measurement data in the field are compared to find the value of the vertical accuracy of DTM ALOS PALSAR. Data height is measured in GNSS-levelling using orthometric height reference fields (Dong et al. 2015, Serrano-Juan et al. 2020). RMSE (z) is a height difference error that occurs at the entire measuring point (see eq. 1).

$$RMSE_{(z)} = \sqrt{\left(\frac{\sum \left(Z_{Data(i)} - Z_{Check(i)} \right)^2}{n} \right)} \tag{1}$$

Z – height value

n – number of measurement points

Z_{Data} – orthometric height on DTM

Z_{Check} – orthometric height measurement

Accuracy (z) is a vertical accuracy value. The Accuracy (z) = 1.96 ∗ RMSE (z), it uses 95% confidence level (Amans et al. 2013, Alganci et al. 2018).

3. Results

As mentioned earlier, DTM is derived from ALOS PALSAR-2 data. The method used is interferometry SAR, and the data set used ALOS PALSAR-2, 2018. The process carried out is the vertical accuracy test of the DTM ALOS PALSAR-2 using a comparison method with GNSS-levelling data in August 2018. DTMs are extracted using three different height reference fields: EGM 1996, EGM 2008, and WGM 2012.
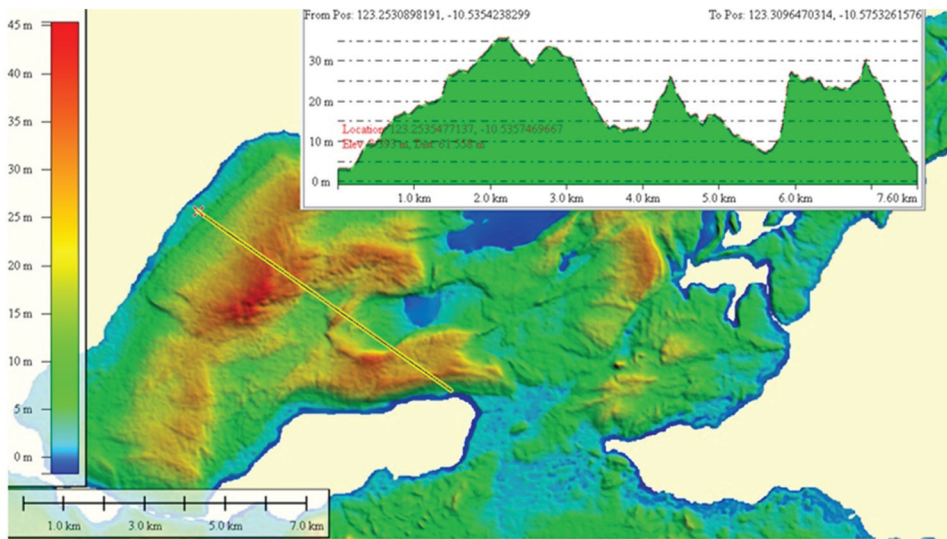

Fig. 4. *Cross-section section profile in the highland area.*

The vertical accuracy-test included the cross-section generation and the height-difference test on the field measurements. Cross-section profile generation can be used to determine the condition of the cross-section profile topography. This cross-section profile is needed to determine the appearance of height errors in the DTM. This cross-section profile is carried out in areas with field measurement data; then, the DTM vertical accuracy test is done by comparing it to field measurements, which are in the form of GNSS-levelling results, see Fig. 4 and Fig. 5. Cross-section profile generation is carried out in the lake and lowlands to the highlands. It uses to identify the topographic variations in the area.
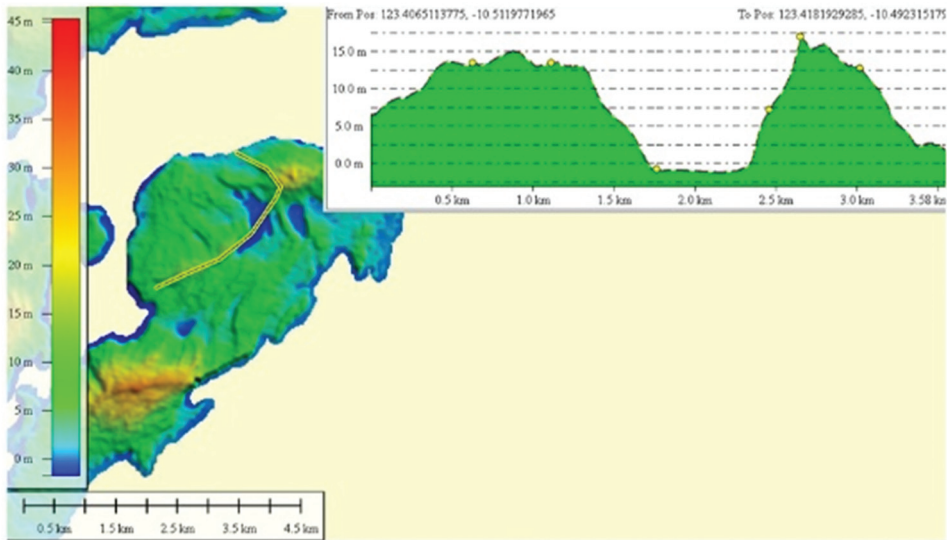
Fig. 5. *Cross-section profile across the lake, lowland, and highland area.*

DTM accuracy test is done by comparing the results of GNSS-levelling measurements in the field. Two locations are tested: areas with high topography (highland) and areas with low topography (lowland). This test used ten height points. The test results can be seen in Table 1.

Table 1. *Vertical accuracy-test of DTM ALOS PALSAR-2 in lowland.*

No	DTM96 (m)	DTM08 (m)	DTM12 (m)	GNSS-levelling (m)	DTM08–DTM96 (m)	DTM12–DTM96 (m)	DTM12–DTM08 (m)	DTM12–GL (m)	DTM08–GL (m)	DTM96–GL (m)
t01	3.54	3.16	4.48	5	−0.382	0.929	1.311	0.525	1.836	1.454
t02	4.11	3.71	5.01	5.4	−0.399	0.903	1.302	0.387	1.689	1.290
t03	3.84	3.44	4.73	6.2	−0.401	0.888	1.290	1.469	2.759	2.358
t04	3.77	3.37	4.68	6.4	−0.399	0.910	1.309	1.719	3.029	2.630
t05	3.88	3.48	4.79	6.8	−0.397	0.914	1.312	2.008	3.320	2.922
t06	4.21	3.82	5.12	7.2	−0.398	0.906	1.304	2.080	3.384	2.986
t07	4.69	4.28	5.55	7.7	−0.404	0.869	1.273	2.145	3.417	3.013
t08	5.31	4.91	6.2	8	−0.406	0.888	1.295	1.798	3.092	2.687
t09	5.88	5.48	6.74	8.3	−0.401	0.864	1.265	1.555	2.819	2.419
t10	6.3	5.91	7.17	8.9	−0.386	0.876	1.259	1.731	2.990	2.605
							sum	15.417	28.336	24.363
							RMSE(z)	1.541	2.834	2.436

DTM96 = DTM using EGM 1996
DTM08 = DTM using EGM 2008
DTM12 = DTM using WGM 2012
GNSS-levelling is field measurement
DTM08–DTM96 = height different between DTM08 with DTM96
DTM12–DTM08 = height different between DTM12 with DTM08
DTM12–DTM96 = height different between DTM12 with DTM96
DTM12–GL= height different between DTM12 with field measurement
DTM08–GL= height different between DTM08 with field measurement
DTM96–GL= height different between DTM96 with field measurement

Based on the vertical accuracy test results in Table 1, the RMSE (z) between DTM12 (WGM 2012) and field measurements is 1.541 m. The field measurement uses GNSS-levelling. The RMSE (z) between DTM08 (EGM 2008) and field measurements is 2.834, and RMSE (z) between DTM96 (EGM 1996) and field measurements is 2.436. The three DTMs have relatively low height differences because the topography of this region is relatively flat.

The average height difference will increase if the topography is not flat. DTM (EGM 2008) has a relatively stable high difference for regions with higher topography, while DTM (EGM 1996) has a better quality for relatively flat topographic areas. The test site is located south of Lake Oemasapoka, one of the saltwater lakes in the Rote Dead Sea area. Fig. 6 shows the study area and height points in the lowland.

Fig. 6. *Study area and height points in lowland.*

There are 10 points used in this test. All these points are measurement points for the height of the road south of Lake Oemasapoka. Measurement of these points is done with GNSS-levelling; then, the DTMs using the EGM 1996, EGM 2008, and WGM 2012 height reference fields are compared with the high point in the field. Table 2 can be seen from the DTM height difference test (EGM 1996, EGM 2008, and WGM 2012). The testing area in the highland is located west of the Rote Dead Sea area; see Fig. 7.

This region is located on a higher topography, and this test also uses 10 test points. In this region, the elevations of WGM 2012 are higher than that of the

field data. The RMSE (z) between EGM 2008 and field measurements is 1.201 m; the RMSE (z) between WGM 2012 and field measurements is 1.185 m, and the RMSE (z) between EGM 1996 and field measurements is 1.432 m.

Fig. 7. *Study area and height points in highland.*

Next, the vertical test was carried out by combining the data on the highlands and the lowlands. The mean of RMSE(z) at DTM is 1.363348 m for WGM 2012, 2.017284 m for EGM 2008, and 1.934208 m for EGM 1996. In general, WGM 2012 is recommended for use as a reference for altitude fields, especially in Rote Island, because it has the smallest difference in height from field measurements. The vertical accuracy calculation results in Table 1 and Table 2 are still in RMSE (z). These results need to be checked on the map scale's suitability according to a specific vertical standard and a certain confidence level. The utilization of maps using DTM is influenced by the type of map scale used.

Table 2. *Vertical accuracy-test of DTM ALOS PALSAR-2 in highland.*

No	DTM96 (m)	DTM08 (m)	DTM12 (m)	GNSS-levelling (m)	DTM08–DTM96 (m)	DTM12–DTM96 (m)	DTM12–DTM08 (m)	DTM12–GL (m)	DTM08–GL (m)	DTM96–GL (m)
t11	35.657	36.220	36.897	40.2	0.563	1.240	0.676	3.303	3.980	4.543
t12	39.324	39.881	40.547	40.4	0.557	1.223	0.666	0.147	0.519	1.076
t13	39.879	40.456	41.124	40.6	0.578	1.245	0.667	0.524	0.144	0.721
t14	41.678	42.246	42.904	41.1	0.568	1.225	0.657	1.804	1.146	0.578
t15	42.856	43.421	44.084	41.6	0.565	1.228	0.663	2.484	1.821	1.256
t16	43.089	43.601	44.263	42	0.512	1.173	0.662	2.263	1.601	1.089
t17	41.636	42.203	42.891	42.8	0.567	1.255	0.688	0.091	0.597	1.164
t18	42.284	42.846	43.520	43.3	0.562	1.236	0.674	0.220	0.454	1.016
t19	42.765	43.327	43.993	43.7	0.562	1.228	0.666	0.293	0.373	0.935
t20	42.358	42.925	43.578	44.3	0.567	1.220	0.653	0.722	1.375	1.942
							sum	11.850	12.010	14.321
							RMSE(z)	1.185	1.201	1.432

DTM96 = DTM using EGM 1996
DTM08 = DTM using EGM 2008
DTM12 = DTM using WGM 2012
GNSS-levelling is field measurement
DTM08–DTM96 = height different between DTM08 with DTM96
DTM12–DTM08 = height different between DTM12 with DTM08
DTM12–DTM96 = height different between DTM12 with DTM96
DTM12–GL= height different between DTM12 with field measurement
DTM08–GL= height different between DTM08 with field measurement
DTM96–GL= height different between DTM96 with field measurement

4. Discussion

In this paper, the vertical accuracy test for DTM is carried out with global standards and applied to various DTM data sources (Richard and Ogba 2018). DTM testing in active tectonic areas with high vertical deformation, such as in Rote, is needed to determine the DTM quality. Areas with earthquake potential require an up-to-date DTM every year (Alganci et al. 2018). The use of global DEMs with old-acquisition will affect the quality of the primary and thematic maps used (Riad, Lumbn-Gaol, Wicaksono, and Pranadita, 2018). High tectonic areas like Rote are no longer optimal in mapping using old-acquisition DEMs such as SRTM, X SAR, ASTER GDEM, and other global DEMs (Tighe and Chamberlain 2009, Amans et al. 2013). DTM in high tectonic areas requires updating DTM every 1–2 years. The latest DTM can be extracted from the latest satellite imagery, such as ALOS PALSAR-2. Every latest DTM that is extracted needs to be tested for vertical accuracy by comparing it with GNSS-levelling measurements (Elkhrachy 2016). This measurement should be carried out in the road area because it is also useful in road monitoring and measurement time efficiency for a large area.

It appears impossible to compare the results obtained with other authors' results since other researchers' investigations were performed differently. Overall, mapping in Indonesia, which has a large area, prioritizes using a map scale of 1:25,000. The vertical accuracy test results in the Rote area are equivalent to a map scale of 1:25,000, with a 95% confidence level. The reason for the equivalent of the map with a scale of 1:25,000 is that the results of the RMSE (z) all tests meet the requirements according to the Indonesian mapping standards and the American Society for Photogrammetry and Remote Sensing (ASPRS) 2014 (ASPRS 2014). This vertical accuracy test results in the Rote area are adjusted to Indonesian and global mapping standards. The results of the vertical accuracy-test can be seen in Table 3.

Table 3. *Vertical accuracy-test based on the map scale.*

No	Study area and height reference field	RMSE(z)	L.E. (90)	Vertical accuracy (90)	L.E. (95)	Vertical accuracy (95)
2	Rote lowland (WGM 2012)	1,541	2,5424959	class 2 (1:10,000)	3,02036	class IX
3	Rote lowland (EGM 2008)	2,834	4,6758166	class 3 (1:10,000)	5,55464	class IX
4	Rote lowland (EGM 1996)	2,436	4,0191564	class 3 (1:10,000)	4,77456	class IX
5	Rote highland (WGM 2012)	1,185	1,9551315	class 1 (1:10,000)	2,3226	class VIII
6	Rote highland (EGM 2008)	1,201	1,9815299	class 1 (1:10,000)	2,35396	class VIII
7	Rote highland (EGM 1996)	1,432	2,3626568	class 2 (1:10,000)	2,80672	class VIII

L.E. = Linear Error

Indonesian mapping standards are based on US NMAS & Perka-BIG no 15/2014 (BIG 2020). Height mapping uses a 90% confidence level. Mapping for a larger scale refers to the ASPRS 2014 accuracy standards with a 95% confidence level (ASPRS 2014). Based on Table 3, the vertical accuracy test in the Rote lowland corresponds to class 2 and class 3 on a scale of 1:10,000. The vertical accuracy test results in the Rote highland correspond to class 1 and class 2 on a scale of 1:10,000. The ALOS PALSAR-2 DTM vertical accuracy test results can be used for mapping scales of 1:10,000 – 1:25,000 in Rote.

Vertical accuracy DEM is affected by the input data type used for extraction (Krauß 2018). ALOS PALSAR-2, which has an L band, can produce DTM with higher vertical accuracy than the C and X band SAR images. This condition is due to the L band penetration, which approaches the ground in dense vegetation. With a lot of savanna and steppe with minimal vegetation, the Rote area will be more suitable for using ALOS PALSAR-2 imagery in DTM extraction.

EGM 1996, EGM 2008, and WGM 2012 in Indonesia dramatically determine the quality of vertical accuracy in high mapping. Indonesia's large area with high tectonic deformation and various volcanic activities can affect the mapping's dynamic height system (Susetyo et al. 2014). Further research is suggested for studies related to mapping and geodynamic characteristics of the height system's influence used for the latest DTM, extracted every 1–2 years.

The vertical accuracy evaluation results in the Rote region will impact the national scale and decision-makers and are also useful globally. This utilization is in the form of a study of world seismicity characteristics because the southern region of Rote is a meeting of the Indo-Australian Plate and the Eurasian Plate (Julzarika et al. 2018). Besides, it also has an impact on disaster mitigation related to seismic dynamics in the Asia-Australia-Pacific region. DTM vertical accuracy evaluation can be applied globally in monitoring the quality of primary geospatial information in a country that does not have high mapping standards.

5. Conclusion

For lowland areas in the Rote archipelago, the vertical accuracy of DTM ALOS PALSAR-2 is recommended for use with WGM 2012. The mean of RMSE(z) at DTM is 1.363348 m for WGM 2012, 2.017284 m for EGM 2008, and 1.934208 m for EGM 1996. The WGM 2012, as a high field reference, especially on Rote Island, is recommended because it has a more significant height difference from the field measurements. EGM 1996, as a reference field, is highly accurate because the height difference from field data is closer to the height difference in WGM 2012. EGM 2008 is not recommended for use as a height reference field in the Rote Islands.

For highland areas, the vertical accuracy of DTM ALOS PALSAR-2 is recommended for use with the WGM 2012. The RMSE (z) in height at DTM is 1.185 m for WGM 2012, 1.201 m for EGM 2008, and 1.432 m for EGM 1996. EGM 1996 can be used for the Rote Islands' highland areas, but EGM 2008 is not recommended as a height reference field for use in the archipelago. The vertical accuracy test in the Rote lowland corresponds to class 2 and class 3 on a scale of 1:10,000. The vertical accuracy test results in the Rote highland correspond to class 1 and class 2 on a scale of 1:10,000. The ALOS PALSAR-2 DTM vertical accuracy test results can be used for mapping scales of 1:10,000 – 1:25,000 in Rote.

References

Albayrak, M., Özlüdemir, M. T., Aref, M. M., Halicioglu, K. (2020): Determination of Istanbul geoid using GNSS/levelling and valley cross levelling data, Geodesy and Geodynamics, Vol. 11, Issue 3, May 2020, 163–173.

Alganci, U., Besol, B., Sertel, E. (2018): Accuracy Assessment of Different Digital Surface Models, ISPRS International Journal of Geo-Information, 7(3), 114.

Amans, O., Beiping, W., Ziggah, Y. (2013): Assessing Vertical Accuracy of SRTM Ver 4.1 and ASTER GDEM Ver 2 Using Differential GPS Measurements – Case Study in Ondo State Nigeria, International Journal of Scientific and Engineering Research, 4(12), 523–531.

Arai, Y. (2019): Pre-treatment for preventing degradation of measurement accuracy from speckle noise in speckle interferometry, Measurement, 136, 36–41.

Arefi, H., D'Angelo, P., Mayer, H., Reinartz, P. (2009): Automatic generation

of digital terrain models from Cartosat-1 stereo images, ISPRS – International Archives of the Photogrammetry Remote Sensing and Spatial Information Sciences, 83(1–4–7), 1–6.

ASPRS (2014): ASPRS Accuracy Standards for Digital Geospatial Data, The American Society for Photogrammetry and Remote Sensing.

Azeez, M. H., Abdulkareem, I. (2019): Accuracy Assessment of Digital Elevation Model (DEM) Data Obtained from ASTER Satellite in Flat Land, IOP Conference Series: Materials Science and Engineering, 518(2).

Balmino, G., Bonvalot, S. (2016): Gravity Anomalies, Encyclopedia Geodesy, International Association of Geodesy.

Balmino, G., Vales, N., Bonvalot, S., Briais, A. (2012): Spherical harmonic modeling to ultra-high degree of Bouguer and isostatic anomalies, Journal of Geodesy, 86(7), 499–520.

Barthelmes, F. (2013): Definition of Functionals of the Geopotential and their Calculation from Spherical Harmonic Models: Theory and formulas used by the calculation service of the International Centre for Global Earth Models (ICGEM), Scientific Technical Report STR09/02, Revised Edition, January 2013, Geo Forschung Zentrum Potsdam.

Barthelmes, F. (2014): Global Models, In: Grafarend, E. (ed.), Encyclopedia of Geodesy, Springer International Publishing, 1–9.

Bayoud, F. A., Sideris, M. G. (2003): Two different methodologies for geoid determination from the ground and airborne gravity data, Geophysical Journal International, 155(3), 914–922.

BIG (2020): Regulation Head of the Geospatial Information Agency number 15/2014 Concerning Basic Map Details Technical Guidelines, Badan Informasi Geospasial (BIG).

Bonvalot, S., Balmino, G., Briais, A., Kuhn, M., Peyrefitte, A., Vales, N., Biancale, R. (2012): World Gravity Map: a set of global complete spherical Bouguer and isostatic anomaly maps and grids, Bureau Gravimétrique International (BGI), EGU General Assembly 2012, held 22–27 April, 2012 in Vienna, Austria, 11091.

Champion, N., Boldo, D. (2006): A robust algorithm for estimating digital terrain models from digital surface models in dense urban areas, Proceedings ISPRS Commission 3 Symposium, Photogrammetric Computer Vision.

Claessens, S. J., Hirt, C. (2013): Ellipsoidal topographic potential: new solutions for spectral forward gravity modeling of topography with respect to a reference ellipsoid, Journal of Geophysical Research: Solid Earth, Vol. 118, 5991–6002.

Devanthéry, N., Crosetto, M., Cuevas-González, M., Monserrat, O., Barra, A., Crippa, B. (2016): Deformation Monitoring Using Persistent Scatterer Interferometry and Sentinel-1 SAR Data, Procedia Computer Science, 100, 1121–1126.

Dong, Y., Chang, H. C., Chen, W., Zhang, K., Feng, R. (2015): Accuracy assessment of GDEM, SRTM, and DLR-SRTM in Northeastern China, Geocarto International, 30(7), 779–792.

Drewes, H., Kuglitsch, F., Adám, J. (2016): The Geodesists Handbook 2016, Journal of Geodesy, 90 (10), 907–1205.

Elkhrachy, I. (2016): Vertical accuracy assessment for SRTM and ASTER Digital Elevation Models: A case study of Najran city, Saudi Arabia, Ain Shams Engineering Journal.

EORC-JAXA (2018): Type of sensor, Retrieved from: https://www.eorc.jaxa.jp/en/hatoyama/experience/rm_kiso/mecha_sensortype_e.html, Japan Aerospace Exploration Agency.

ESA (2020): Grace Satellites, Retrieved from: https://earth.esa.int/web/guest/missions/3rd-party-missions/current-missions/grace, European Space Agency.

Gallant, J. C., Read, A. M., Dowling, T. I. (2012): Removal of Tree Offsets From Srtm and Other Digital Surface Models, ISPRS – International Archives of the Photogrammetry, Remote Sensing and Spatial Information Sciences, XXXIX-B4 (September), 275–280.

Gesch, D. B., Oimoen, M. J., Evans, G. A. (2014): Accuracy assessment of the U.S. Geological Survey National Elevation Dataset, and comparison with other large-area elevation datasets: SRTM and ASTER, Open-File Report, 18.

Hirt, C., Kuhn, M. (2012): Evaluation of high-degree series expansions of the topographic potential to higher-order powers, Journal Geophysical Research (JGR) – Solid Earth.

Hirt, C., Kuhn, M., Featherstone, W. E., Goettl, F. (2012): Topographic/isostatic evaluation of new-generation GOCE gravity field models, Journal of Geophysical Research – Solid Earth, B05407.

Hofmann-Wellenhof, B., Moritz, H. (2006): Physical Geodesy, Second edition, Springer, Wien, New York.

Ince, E. S., Barthelmes, F., Reißland, S., Elger, K., Förste, C., Flechtner, F., Schuh, H. (2019): ICGEM – 15 years of successful collection and distribution of global gravitational models, associated services, and future plans, Earth System Science Data, 11, 647–674.

JAXA (2019): ALOS Data Users Handbook Revision C. Aerospace, (March), 158, Retrieved from: http://www.eorc.jaxa.jp/ALOS/en/doc/fdata/ALOS_HB_RevC_EN.pdf.

Julzarika, A., Dewi, E. K. (2018): Uji Ketelitian DTM ALOS PALSAR Terhadap Pengukuran Kombinasi DGNSS-Altimeter, Jurnal Penginderaan Jauh Dan Pengolahan Data Citra Digital, 15(1), 11–24 (in Indonesian).

Julzarika, A., Djurdjani, D. (2018): DEM classifications: opportunities and potential of its applications, J. Degrade. Min. Land Manage, 5(53).

Julzarika, A., Laksono, D. P., Subehi, L., Dewi, E. K., Kayat, K., Sofiyuddin, H. A., Nugraha, M. F. I. (2018): Comprehensive integration system of saltwater environment on Rote Island using a multidisciplinary approach, J. Degrade. Min. Land Manage, 5(53), 2502–2458.

Krauß, T. (2018): A New Simplified DSM to DTM Algorithm, DSM to DTM step.

Laksono, D., Julzarika, A., Subehi, L., Sofiyuddin, H. A., Dewi, E. K., Nugraha, M. F. I. (2019): Expedition Oe: A Visual-storytelling map on Rote Island's Lakes, Journal of Geospatial Information Science and Engineering, 1(2), 87–93.

Lanari, R., Mora, O., Manunta, M., Mallorquí, J. J., Berardino, P., Sansosti, E. (2004): A small-baseline approach for investigating deformations on full-resolution differential SAR interferograms, IEEE Transactions on Geoscience and Remote Sensing, 42(7), 1377–1386.

Lazecký, M., Hlaváčová, I., Martinovič, J., Ruiz-Armenteros, A. M. (2018): Accuracy of Sentinel-1 Interferometry Monitoring System based on Topography-free Phase Images, Procedia Computer Science, 138, 310–317.

Li, Z., Zhu, Q., Gold, C. (2004): Digital terrain modeling: Principles and methodology, CRC Press.

Maune, D. F., Nayegandhi, A. (2018): Digital Elevation Model Technologies and Applications: The DEM Users Manual, American Society for Photogrammetry and Remote Sensing.

Monserrat, O., Crosetto, M., Luzi, G. (2014): A review of ground-based SAR interferometry for deformation measurement, ISPRS Journal of Photogrammetry and Remote Sensing, 93, 40–48.

Moudrý, V., Lecours, V., Gdulová, K., Gábor, L., Moudrá, L., Kropáček, J., Wild, J. (2018): On the use of global DEMs in ecological modeling and the accuracy of new bare-earth DEMs, Ecological Modelling, 383, 3–9.

Mukherjee, S., Joshi, P. K., Mukherjee, S., Ghosh, A., Garg, R. D., Mukhopadhyay, A. (2012): Evaluation of vertical accuracy of open source Digital Elevation Model (DEM), International Journal of Applied Earth Observation and Geoinformation, 21 (1), 205–217.

NASA (2018): Remote Sensors, Retrieved from: https://earthdata.nasa.gov/user-resources/remote-sensors, The National Aeronautics and Space Administration.

Pavlis, N. K., Holmes, S. A., Kenyon, S. C., Factor, J. K. (2012): The development and evaluation of the Earth Gravitational Model 2008 (EGM2008), Journal of geophysical research: solid Earth, Vol. 117, Issue B4, American Geophysical Union.

Pirotti, F. (2010): Assessing a template matching approach for tree height and position extraction from lidar-derived canopy height models of Pinus pinaster stands, Forests, 1(4), 194–208.

Reale, D., Serafino, F., Pascazio, V. (2009): An accurate strategy for 3D ground-based SAR imaging, IEEE Geoscience and Remote Sensing Letters, 6(4), 681–685.

Riadi, B., Lumbn-Gaol, Y. A., Wicaksono, B., Pranadita, S. (2018): Vertical Accuracy Assessment of DSM from TerraSAR-X and DTM from Aerial Photogrammetry on Paddy Fields – Karawang, Indonesia, Advances in Science, Technology and Engineering Systems Journal, Vol. 3, No. 4, 187–192.

Richard, J. Ogba, C. (2018): Analysis of Accuracy of Differential Global Positioning System (DGPS) and Google Earth Digital Terrain Model (DTM)

Data using Geographic Information System Techniques, FIG Working Week 2017, Surveying the world of tomorrow – From digitalisation to augmented reality, Helsinki, Finland.

Rucci, A., Ferretti, A., Monti Guarnieri, A., Rocca, F. (2012): Sentinel-1 SAR interferometry applications: The outlook for sub-millimeter measurements, Remote Sensing of Environment, 120, 156–163.

Satge, F., Denezine, M., Pillco, R., Timouk, F., Pinel, S., Molina, J., Bonnet, M. P. (2016): Absolute and relative height-pixel accuracy of SRTM-GL1 over the South American Andean Plateau, ISPRS Journal of Photogrammetry and Remote Sensing, 121.

Schuman, G. J. P., Bates, P. D. (2019): Commentary: The need for a high-accuracy, open-access global DEM, Frontiers in Earth Science, 7, 1–4.

Serrano-Juan, A., Pujades, E., Vázquez-Suñè, E., Crosetto, M., Cuevas-González, M. (2020): Leveling vs. InSAR in urban underground construction monitoring: Pros and cons., Case of la sagrera railway station (Barcelona, Spain), Engineering Geology, 218, 1–11.

Susetyo, D. B., Syetiawan, A., Octariady, J. (2014): Geometric Accuracy Comparison between High Resolution Satellite Imagery and Aerial Photo for Large Scale Topographic Mapping, National seminar on Remote Sensing 4th.

Szostak-Chrzanowski, A. (2006): The interdisciplinary approach to deformation analysis in engineering, mining, and geosciences projects by combining monitoring surveys with deterministic modelling, Part 1, Technical Sciences, University of Warmia and Mazury in Olsztyn, nr 9, 147–172.

Tighe, L., Chamberlain, D. (2009): Accuracy Comparison of the SRTM, ASTER, NED, NEXTMAP® USA Digital Terrain Model Over Several USA Study Sites, ASPRS/MAPPS 2009 Fall Conference, November 16–19, San Antonia, Texas.

Trisakti, B., Julzarika, A. (2011): DEM generation from stereo ALOS PRISM and its quality improvement, International Journal of Remote Sensing and Earth Sciences, 8, 41–48.

Turcotte, D., Schubert, G. (2014): Geodynamics, 3rd edition, Cambridge University Press.

Venera, J., Anton, F., Irina, K., Alena, Y. (2016): SAR Interferometry Technique for Ground Deformation Assessment on Karazhanbas Oilfield, Procedia Computer Science, 100, 1163–1167.

Zrinjski, M., Barković, Đ., Matika, K. (2019): Development and Modernization of GNSS, Geodetski list, 73 (96), 1, 45–65.

Procjena visinske točnosti digitalnog modela terena (DMT) ALOS PALSAR-2 u području Rote Dead Sea – Indonezija

SAŽETAK. *Procjenu visinske točnosti neophodno je obaviti kako bi se utvrdila kvaliteta DMT-a. Ta će kvaliteta utjecati na vrstu mjerila i korištenje DMT-a. U studiji se koriste podaci iz DMT-a ALOS PALSAR-2. Ova studija procjenjuje visinsku točnost DMT-a ALOS PALSAR-2 s različitim referentnim područjima visine u području Rote Dead Sea, Indonezija. Svaki DMT izrađen je uz pomoć EGM 1996, EGM 2008 i WGM 2012. Tri DMT-a, koja se temelje na referentnim područjima visine, imat će različite ortometrijske visine; zato je potrebna procjena visinske točnosti kako bi se odredila kvaliteta ta tri DMT-a. Oni se uspoređuju s terenskim mjerenjima dobivenima GNSS-niveliranjem. Ovo ispitivanje provodi se u nizinskim i brdskim područjima koristeći 10 testnih točaka. Za nizinsko područje, RMSE (z) u visini na DMT-u je 1,363 m za WGM 2012, 2,017 m za EGM 2008 i 1,934 m za EGM 1996. Za brdsko područje, RMSE (z) u visini na DMT-u je 1,185 m za WGM 2012, 1,201 m za EGM 2008 i 1,432 m za EGM 1996. DMT-WGM 2012 i DMT-EGM 1996 preporučuju se za korištenje u tom području jer imaju veću visinsku točnost. Ispitivanje visinske točnosti u nizinskom području otoka Rote odgovara klasi 2 i klasi 3 u mjerilu 1:10 000. Ispitivanje visinske točnosti u brdskom području otoka Rote odgovara klasi 1 i klasi 2 u mjerilu 1:10 000. Rezultati ispitivanja visinske točnosti DMT-a ALOS PALSAR-2 mogu se koristiti za mjerila kartiranja 1:10 000 – 1:25 000 na otoku Rote.*

Ključne riječi: ispitivanje visinske točnosti, EGM 1996, EGM 2008, WGM 2012, DMT ALOS PALSAR-2.